PROSPECTS OF EBW EMISSION DIAGNOSTICS AND EBW HEATING IN SPHERICAL TOKAMAKS

V. F. Shevchenko[1], *Y. Baranov*[1], *M. O'Brien*[1], *A. D. Piliya*[2], *J. Preinhaelter*[3], *A. N. Saveliev*[2], *E. N. Tregubova*[2], *F. Volpe*[1]

[1]EURATOM/UKAEA Fusion Association, Culham Science Centre, Abingdon, Oxon, OX14 3DB, UK
[2]Ioffe Institute, Politekhnicheskaya 26, 194021 St.Petersburg, Russia
[3]EURATOM/IPP.CR Association, Institute of Plasma Physics, 182 21 Prague, Czech Republic

e-mail: vladimir.shevchenko@ukaea.org.uk

Extensive studies of plasma EBW emission have been conducted over the past few years in MAST and NSTX. Thermal emission observations from overdense plasmas cover the frequency range from the fundamental up to the 6th EC harmonic. In general, observed emission spectra are consistent with the theory of mode coupling and EBW propagation in ST plasmas. However, some particular features of EBW emission still require a proper explanation. EBW excitation and propagation in ST plasmas has been modeled for a wide range of frequencies and plasma scenarios. The main aim of this modelling was the identification of the optimal frequency and launch configuration for plasma heating and current drive in STs, taking into account also experimental EBW emission observations. Predictions for future EBW heating and current drive performance in STs together with the uncertainties in our estimates are presented and discussed.

INTRODUCTION

Conventional ECE diagnostics and ECRH methods cannot be used in spherical tokamaks (STs) because of the specific plasma parameters. Typically the plasma is well overdense in STs, i.e. $\omega_{pe} >> \omega_{ce}$, where ω_{pe} and ω_{ce} are the electron plasma and electron cyclotron frequencies, respectively. In such plasmas the core appears to be inaccessible for conventional electromagnetic modes in the range of frequencies corresponding to the first few EC harmonics. This is primarily because EC resonances in the core plasma are completely obscured by cut-offs. Electron Bernstein waves (EBW), unlike the ordinary (O) mode and the extraordinary (X) mode, experience strong damping even at high harmonics of the EC resonance frequency. EBWs do not have any density cut-offs inside the plasma and can, therefore, access plasmas of arbitrary densities for frequencies above ω_{ce}. These features of EBWs present the possibility of efficient means for ECE diagnostics and ECRH in high beta plasmas, particularly in STs, where the X-mode and O-mode propagation into the plasma can only be assured at high EC harmonics leading to weak damping of these modes inside the plasma.

EBWs are predominantly electrostatic waves and they cannot propagate in vacuum. However, EBWs can be coupled to the vacuum electromagnetic waves

via mode conversion mechanisms. These mechanisms allow the thermal EBW emission to escape the plasma and inversely EBWs can be excited within the plasma with the externally launched X or O modes. By the reciprocity theorem both processes are completely symmetrical until the non-linear effects of plasma-wave interaction become significant.

2. EBW EMISSION STUDIES

On MAST [1] the EBW emission is studied with a frequency scanning heterodyne radiometer [2], which covers three frequency bands 16-26 GHz, 26-40 GHz and 40-60 GHz. The full frequency scan, which takes 0.32 ms with fast sampling or 0.64 ms with a standard sampling rate, is arranged in 32 frequency steps for each frequency band. As a result, the plasma emission spectrum is measured over 96 frequencies during the shot. The majority of experiments have been conducted with the antenna viewing optimised for the B-X-O mode conversion for the frequencies within the radiometer range. However, the B-X mode converted emission was also studied in MAST.

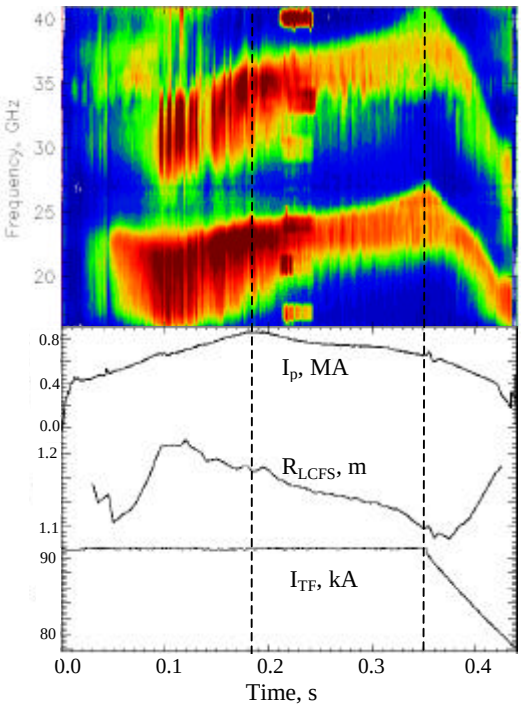

Fig.1 EBW emission spectrogram measured during high density plasma shot #7798 in MAST. Red areas correspond to higher emission intensity. ECRF power was injected at 0.21-0.24 s.

An experimentally measured spectrogram (Fig. 1) illustrates the main features of the B-X-O mode converted emission in MAST. As soon as the plasma density reaches the value required for B-X-O conversion, the EBW signals from different ω_{ce} harmonics appear in the spectrum. Here the emission from the first two harmonics (and partly from the third) is clearly seen during the initial stage of the discharge. The dark gaps in the spectrum always separate neighbouring harmonics. These gaps correspond to the plasma layers, where cyclotron harmonics are coincident with the UHR [3]. The spectral maxima of harmonics move up in frequency during this phase of the discharge because the

plasma current ramps up, while the toroidal field remains constant. At about 100 ms the emission from the second harmonic has a well-pronounced jump down in frequency and simultaneous increase in intensity. At this time the plasma enters the ELMy H-mode.

The associated increase in edge density gradient enhances the mode conversion efficiency resulting in the increase of the emission intensity at all harmonics. The L-H transition also shifts the mode conversion layer from the bulk plasma outwards into the lower magnetic field resulting in the frequency jump down. At about 200 ms the plasma falls out of H-mode resulting in the decrease of the EBW emission intensity and then the plasma is sustained in L-mode until the end of the shot. During that period of time no significant changes in emission intensity occur because the electron temperature remains almost constant. The steady drift of the spectrum to higher frequencies is related to the plasma current ramp up from 0 to 180 ms and plasma compression started at 100 ms. At the end of the toroidal field flattop at 350 ms the EBW emission spectrum

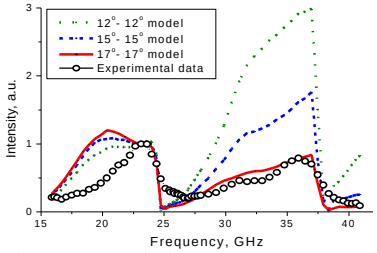

Fig.2 EBW emission spectrum measured during L-mode in MAST, shot #7798, 0.24 s, and modelling results for different viewing angles.

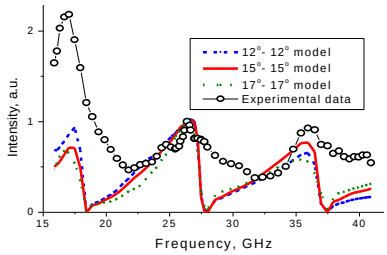

Fig.3 EBW emission spectrum measured during H-mode in MAST, shot #7786, 0.24 s, and modelling results for different viewing angles.

quickly drifts down over the frequency range. Such behaviour is consistent with modelling of thermal EBW emission from the ST plasma. A special code has been developed for EBW spectral analysis [4]. The model includes the gaussian optics formalism for the receiving antenna, interference and aperture effects from the vacuum window, the 1D full wave treatment of the mode coupling at the plasma boundary, EBW ray-tracing and emitted power integration procedure. The modelling results are compared with experimental data in Fig. 2. Usually the EBW emission spectrum measured in L-mode has a well-pronounced sawtooth structure [3] separating emission from different harmonics. Magnetic equilibrium reconstruction obtained from EFIT and electron temperature and density profiles measured with Thomson scattering (TS) are used in the estimates of the spectrum of plasma emission. The modelling of the spectrum has been conducted for a few sets of antenna viewing angles. The curve corresponding to 17° poloidal and 17° toroidal viewing angles shows the best agreement with the experimentally measured spectrum. This is consistent with the antenna configuration within the accuracy of the experimental set-up. A noticeable

disagreement at lower frequencies can be due to the presence of low density fluctuations outside the separatrix, which were not accounted for in the model. Simulated spectra also show deeper drops of the intensity between harmonics than the experimental data. That can be partly attributed to the stray radiation, which is always present in a reflecting tokamak vessel.

The emission spectrum and its dynamics are completely different during H-mode. Theory predicts that the sawtooth character of the EBW spectrum should not change after the L-H transition. It should become even more pronounced during H-mode with the increased level of EBW emission due to the enhancement of the mode conversion efficiency (see modelling results in Fig. 3). Experimental results confirm this prediction but only for the initial stage of the H-mode phase. The emission intensity is typically enhanced by a few times immediately after the L-H transition and the spectrum has a pronounced sawtooth structure [5]. During the next 10-20 ms after the L-H transition the spectrum becomes "triangular" while modelling still predicts a sawtooth-like spectrum (Fig. 3). Moreover, if the plasma is sustained in H-mode longer than 30-50 ms the behaviour of the EBW emission changes dramatically. There are two important phenomena observed in high density H-mode [6]. The first one is the inverse EBW intensity modulation with ELMs. It usually appears during the early stage of the H-mode at the second or third EC harmonics. During ELM-free periods $2\omega_{ce}$ emission is suppressed, while the emission from ω_{ce} and $3\omega_{ce}$ harmonics is enhanced. Conversely, the $2\omega_{ce}$ emission quickly recovers during the L-mode phase, when other harmonics are suppressed.

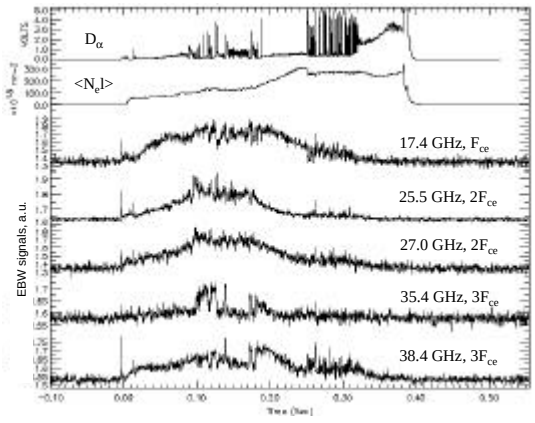

Fig.4 EBW signals suppression during high density H-mode in MAST

The second phenomenon is that the EBW emission intensity gradually decays if the plasma is sustained in H-mode for some time (Fig. 4). The EBW emission decay can be quite substantial, especially at high plasma current (~1 MA) and low TF. In some discharges the emission intensity drops down by a few times and the decrease in intensity can be more pronounced at one particular harmonic. Emission suppression starts from the lower frequency part within each harmonic and then spreads out to higher frequencies. It should be noted that after a giant ELM or a long L-mode phase the emission behaviour comes back to normal. Typically, the decay occurs simultaneously at all frequencies with the time scale of 20-30 ms, which is about half of the energy confinement time in these

discharges. At the same time plasma temperature and density profiles, as measured by multi-point TS, do not exhibit any significant changes. The emission spectrum during this stage is completely different from the modelling (Fig. 3) and from the spectrum measured during L-mode (Fig. 2). Full wave modelling of the O-X-B mode coupling, based on the experimentally measured profiles and EFIT equilibrium, shows that no degradation of the coupling efficiency occurs during the H-mode. In fact, the coupling efficiency must be close to 100% in a wide angular range.

Apparently, both these phenomena can be attributed to the plasma current redistribution initiated by the H-mode. Indeed, the plasma equilibrium is quite different in the L and H mode. In the H-mode, at least, a higher bootstrap fraction must be driven in the gradient zone, close to plasma layers where the mode conversion occurs. The edge current generation in the pedestal region during H-mode has been recently experimentally confirmed on DIII-D [7]. It was reported that during H-mode and QH-mode an edge localised current density of 1-2 MA/m^2 was measured using lithium beam Zeeman polarimetry. The L-mode shows a much smaller current density at the edge. The edge current during H-mode increases the inclination of the magnetic field at the separatrix. The increase is measured to be ~1° with the typical edge pitch angle of 16° in DIII-D. If we assume a similar value of the edge pressure driven current density in MAST the increase of the edge pitch angle can be about 5° because the edge magnetic field is typically five times smaller in MAST. Thus, quite a strong edge localised magnetic perturbation must be expected after the L-H-transition.

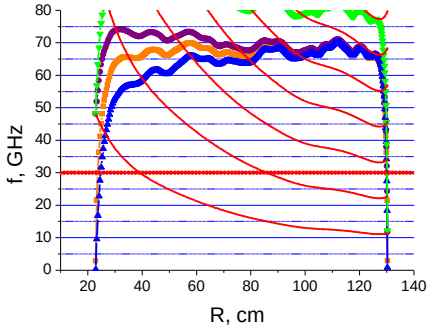

Fig. 5 Midplane cut-off and resonance topology, shot #6141. Edge magnetic well was formed assuming the edge pressure driven current density of 2 MA/m^2.

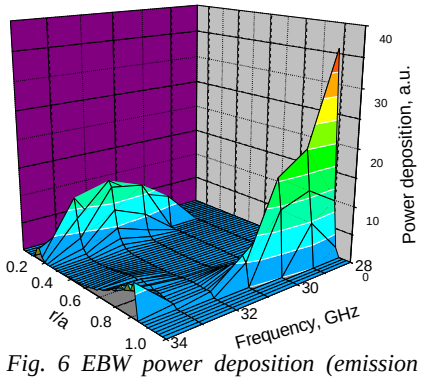

Fig. 6 EBW power deposition (emission origin) for equilibrium shown in Fig. 5. EBW ray-tracing results.

First of all the increase of the edge pitch angle leads to a change of the optimal viewing / launch angle for the O-X-B mode conversion. It will have maximum effect at frequencies whose O-mode cut-off is coincident with the maximum of the pitch angle perturbation. Note, that inverse emission modulation by ELMs was typically observed in MAST plasmas at the 2nd EC harmonic. The pitch angle modulation with ELMs must lead to a coupling

efficiency modulation, which can explain the experimentally observed $2\omega_{ce}$ emission modulation. Secondly, in high beta plasmas a magnetic well (minimum of the total magnetic field) must be formed. Magnetic well formation is experimentally observed on NSTX and MAST in plasmas with beta exceeding ~10%. Such a magnetic well is a result of the routine EFIT magnetic equilibrium reconstruction, which does not include edge current. The edge pressure driven current must increase the depth of the well so that the total magnetic field will gradually increase towards the separatrix. A large enough edge current can form a local magnetic well itself (Fig. 5). EC harmonics become inverted in the outer part of the well, in the sense that the higher field side of harmonics is facing the lower field (outboard) side of the tokamak. Such a non-monotonic behaviour of the magnetic field near the separatrix dramatically changes the EBW trajectories resulting in enhanced peripheral absorption (Fig. 6). Consequently it causes a decrease of the emission intensity primarily from the lower frequency part within each harmonic. As the magnetic well develops the emission suppression should spread over all harmonics. The emission spectrum corresponding to the power deposition in Fig. 6 would be very similar to the experimental one in Fig. 3.

The above discussion shows that the edge pressure driven current could in principle explain the EBW emission behaviour during H-mode in MAST. The possible proof of this hypothesis is to conduct EBW spectral measurements in the range of viewing angles optimal for the expected pitch angles in L-mode and H-mode. At some angles a significant enhancement instead of suppression of the emission must be seen if the hypothesis is true. This experiment would also demonstrate the potential of using EBW diagnostics for pitch angle measurements. The understanding of EBW emission phenomena is of great importance for the future application of EBW heating and current drive in STs.

EBW HEATING EXPERIMENTS ON MAST

The overall aim of the initial EBW (60 GHz) heating experiments in MAST was to conduct commissioning tests of the new steerable antenna, and to obtain preliminary indications of the range of launch angles and plasma parameters over which effective O-X-B coupling may be obtained. A high density plasma scenario has been developed in order to optimise RF power deposition closer to the magnetic axis. In this scenario the density gradient is very steep in the range up to $2 \cdot 10^{19}$ m^{-3} and has a relatively moderate value at higher densities. This allows us to shift the plasma cut-off (O-X conversion layer) by 10-15 cm deeper into the plasma, avoiding interception by the upper EC harmonics.

A toroidal field (TF) scan has been conducted within the range of 60 GHz O-mode cut-off intersections with the 5^{th} and 6^{th} EC harmonics. The TF scan has shown that the EBW emission enhancement during ECRF injection has a well-pronounced maximum when the O-mode cut-off is located at 2/3 of the distance between the 5^{th} and 6^{th} EC harmonics. This scenario with optimised TF has provided some evidence of plasma heating during ECRF power injection. The

heating was not strong, hence, the effect is better seen after averaging over 3 shots. The Fig. 7 indicates a ~10% increase of the total plasma energy (EFIT) during the ECRF pulse with an average injected RF power of ~0.25 MW. The total heating power (NBI + Ohmic) in these shots was about 3 MW.

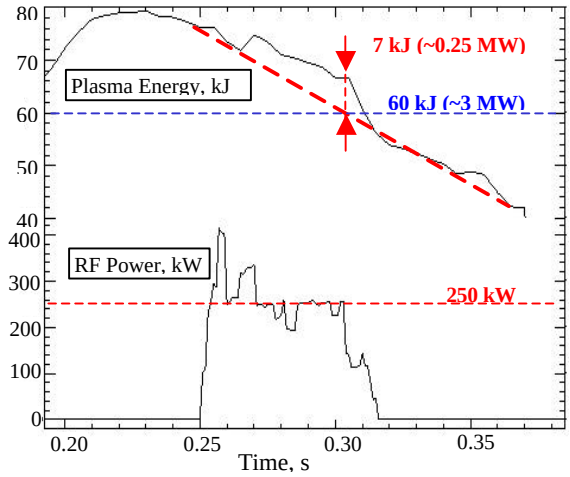

Fig. 7 EBW heating results averaged over 3 plasma shots.

The small heating effects in these experiments can be attributed to antenna misalignment, which was discovered after the experimental campaign. It was found that RF power from some gyrotrons was injected into the plasma with an angular offset of up to 7°. Aiming is critical for the O-X-B mode conversion efficiency. With such an offset the RF power was only partly converted into EBW. On the other hand, such effects as the enhanced EBW emission [6] and total plasma energy increase during RF injection must be related not to the total power injected into the vessel but to the power really converted into the EBW mode. This is a quite encouraging fact suggesting that with the full available power (1.4 MW) launched at the optimal angle one can expect EBW heating effects an order of magnitude stronger.

EBW MODELLING AND PROSPECTS

The right choice of frequency and launch configuration for EBW heating and CD is a key issue for future applications in STs. The propagation and dispersion of EBWs is a complicated function of electron temperature and magnetic field in the plasma. Magnetic field topology in STs is characterised by relatively rapid variations of poloidal and toroidal components over the major radius. This fact makes the task of EBW heating and CD optimisation multi-parametric. Here, we present the results of numerical modelling for one particular plasma scenario, which is considered for future MAST operation. Modelling was conducted in a parametric space including variations of heating frequency over the fundamental and second harmonic, different launch polarisation and vertical position of the launcher. The goal was to find the optimal parameters for off axis CD and for central heating and CD. The EBW excitation in the plasma is considered as a full wave 1D mode-coupling problem in slab geometry. Propagation and absorption of the EBW is computed using the

EBW ray-tracing code [8], which implements the fully electromagnetic, hot plasma dispersion function. The driven currents were estimated using relativistic Fokker-Planck codes [9,10].

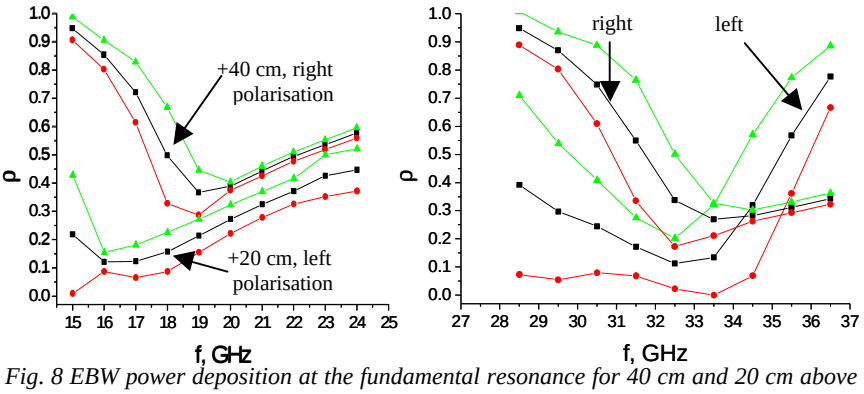

Fig. 8 EBW power deposition at the fundamental resonance for 40 cm and 20 cm above midplane launch (left fig.) and at second harmonic (right fig.) for 30 cm above midplane launch with different polarisations. Squares correspond to the maximum absorption, triangles and circles indicate the range of power deposition.

For each vertical position of the launcher one has a choice of two launch configurations allowing optimal power coupling from the ordinary polarised wave into EBW. We do not consider here the X-B conversion scenario which gives the third launch option. The first launch configuration assumes that the wave is launched in the direction counter to the edge magnetic field and has an almost circular **right-handed** polarisation with the electric field rotating counter to the electron gyration (O-mode). The second launch is in the co-direction to the edge magnetic field with **left-handed** polarisation rotating counter to the electron gyration (O-mode). Choosing the vertical position and the launch option we actually specify the initial $N_{||}$ spectrum for the EBW beam which completely defines further propagation and absorption of the beam. Fig. 8 illustrates the power deposition location computed for fundamental and second harmonic EC resonance in a range of frequencies for two different launch configurations. A very localised absorption at the fundamental harmonic is possible in normalised radii ρ range from 0.35 to 0.55 with frequencies 20-24 GHz while at the second harmonic localised absorption is only possible around $\rho \sim 0.3$ with frequencies >34 GHz. The localisation is typically better with the right polarisation while the left polarisation allows power deposition closer to the magnetic axis.

An interesting possibility is the radial control of the power deposition with one chosen frequency of 18 GHz by variation of the vertical launch position. Fig. 9 illustrates the potential of this method. The left figure shows that with +70 cm off- midplane launch the main power (90%) is deposited between ρ=0.55 and ρ=0.8 with $N_{||} \approx 1$, which is good if broad off-axis CD is required. In the range of launcher positions between 30 and 60 cm the power deposition becomes very broad covering more than half the minor radius. With near midplane launch the

power can be deposited very close to the magnetic axis at ρ ~ 0.1–0.2. $N_{||}$ remains positive for all launcher positions with the left polarisation launch. If we switch polarisation to right or the launcher is moved down below the midplane, which is the same apart from the opposite sign of $N_{||}$, the right figure shows totally different features. For the launcher positions between 5cm and 15 cm the power deposition reveals two maxima with opposite $N_{||}$, so the expected CD efficiency is very poor with such launch due to co- /counter- compensation. In the range from 20 to 40 cm the power deposition is extremely localised at about ρ=0.3 with $N_{||} \approx 0.4$. Further launcher movement leads to a gradual displacement of the absorption zone to the periphery with a moderately broad power deposition profile. The modelling has shown that for efficient central plasma heating and CD the left polarisation is preferable with the launch close to the midplane. For the off-axis CD at ρ ≈ 0.7 – 0.9 the launcher must be placed about 40 cm off midplane (Fig. 8, left) and only the lower frequency part of the harmonic can provide reasonably narrow power deposition.

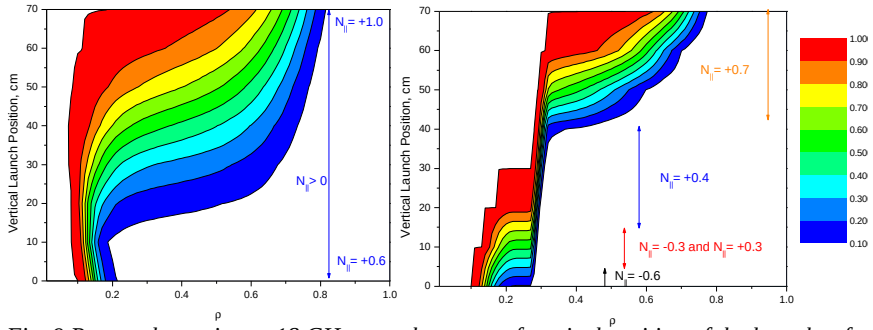

Fig. 9 Power absorption at 18 GHz over the range of vertical position of the launcher for the left (on the left) and right polarisation (on the right). The sign of $N_{||}$ indicates the CD direction.

Current drive by electron Bernstein waves has been demonstrated in the conventional tokamak COMPASS-D, by exploiting X-B mode conversion with the extra-ordinary mode launched from the HFS [11]. The current drive efficiency measured, $\eta_{20} \sim 0.035$ $AW^{-1}m^{-2}$, exceeded that achievable with conventional ECRH for similar plasma parameters. The EBW current drive capability in MAST over the radius has been assessed for a single frequency of 18 GHz. The radial power deposition was varied by variation of polarisation and the launcher position (Fig. 10). Two radial positions ρ≈0.5 and ρ≈0.9 are inaccessible with this frequency at a fixed equilibrium, so 22 GHz and 16 GHz were used for these radii respectively. The strong trapping effects at low aspect ratio reduce the Fisch-Boozer current whilst enhancing the Ohkawa current at large minor radius. As a result, calculations show that the two effects tend to cancel at r/a ~ 0.7 in MAST. Beyond this radius the Ohkawa effect dominates and initial modelling results show that this scheme might be very effective for providing edge current drive in STs.

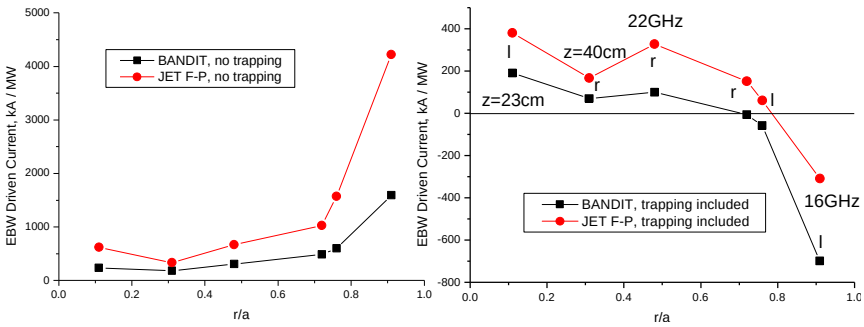

Fig. 10 Predicted EBW CD over radius with 1 MW injected power without trapping (left figure) and including trapping (right figure) effects (preliminary results). f = 18GHz, z= 70cm, except where indicated. r,l indicate right & left polarisation respectively.

In summary we have to conclude that low frequency EBW heating and current drive are preferable in STs. The fundamental resonance frequencies allow efficient CD close to the magnetic axis while second harmonic frequencies are beneficial for off axis CD. Radial power deposition for both harmonics can be controlled by the vertical position of the launcher. The strong harmonic overlap and large field line pitch angle, which can pose difficulties for EBW heating in STs, also present unique diagnostic opportunities. The high sensitivity of the O-X mode conversion efficiency to the angle of incidence at the plasma cut-off (where mode conversion occurs) might provide a means to measure the edge current density profile in STs. In principle, measurement of the optimum angle for B-X-O emission as a function of frequency will directly give the field line pitch angle as a function of plasma density near the plasma edge.

ACKNOWLEDGEMENTS

This work was funded jointly by the United Kingdom Engineering and Physical Sciences Research Council and by EURATOM.

REFERENCES

[1] Darke A.C., et al., Proc. of the 18th Symposium on Fusion Technology, Karlsruhe, Germany, 22-26 August 1994 (Elsevier, Amsterdam, 1995), Vol. 1, p. 799.
[2] Shevchenko V., Proc. 27th EPS, Budapest, Hungary, 2000, P-3.120.
[3] Shevchenko V., Plasma Phys. Reports, Vol. 26, No 12, p.1000 (2000).
[4] Preinhaelter J., et al., Rev. Sci. Instr. (2004) *to be published.*
[5] Shevchenko V., et al., Proc. 28th EPS, Funchal, Madeira, Portugal, 2001, P-3.101.
[6] Shevchenko V., Proc. 15th Topical Conf. on RF Power in Plasmas, 2003, p. 359.
[7] Leonard A.W., et al., Bull. Am. Phys. Soc. 48, 184, (2003).
[8] Tregubova E., et al., Proc. 30th EPS, St. Petersburg, Russia, P-3.203 (2003).
[9] Shoucri M. and Shkarovsky I., Comp. Phys. Comm. **82**, 287 (1994).
[10] O'Brien M. et al, Proc. IAEA TCM on Advances in Simulation and Modelling of Thermonuclear Plasma, Montreal, 527 (1992).
[11] Shevchenko V., et al., Phys. Rev. Lett. 89, 265005-1 (2002).